Analysis of Anatomic and Functional Measures in X-Linked Retinoschisis

Catherine A. Cukras,[1,2] Laryssa A. Huryn,[2] Brett G. Jeffrey,[2] Amy Turriff,[2] and Paul A. Sieving

[1]Division of Epidemiology and Clinical Research, National Eye Institute, National Institutes of Health, Bethesda, Maryland, United States
[2]Ocular Genetics and Visual Function Branch, National Eye Institute, National Institutes of Health, Bethesda, Maryland, United States

Correspondence: Catherine A. Cukras, Division of Epidemiology and Clinical Applications, National Eye Institute, National Institutes of Health, Bethesda, MD 20892, USA; cukrasc@nei.nih.gov.

Submitted: November 20, 2017
Accepted: April 13, 2018

Citation: Cukras CA, Huryn LA, Jeffrey BG, Turriff A, Sieving PA. Analysis of anatomic and functional measures in X-linked retinoschisis. *Invest Ophthalmol Vis Sci*. 2018;59:2841–2847. https://doi.org/10.1167/iovs.17-23297

Purpose. To examine the symmetry of structural and functional parameters between eyes in patients with X-linked retinoschisis (XLRS), as well as changes in visual acuity and electrophysiology over time.

Methods. This is a single-center observational study of 120 males with XLRS who were evaluated at the National Eye Institute. Examinations included best-corrected visual acuity for all participants, as well as ERG recording and optical coherence tomography (OCT) on a subset of participants. Statistical analyses were performed using nonparametric Spearman correlations and linear regression.

Results. Our analyses demonstrated a statistically significant correlation of structural and functional measures between the two eyes of XLRS patients for all parameters. OCT central macular thickness ($n = 78$; Spearman $r = 0.83$, $P < 0.0001$) and ERG b/a ratio ($n = 78$; Spearman $r = 0.82$, $P < 0.0001$) were the most strongly correlated between a participant's eyes, whereas visual acuity was less strongly correlated ($n = 120$; Spearman $r = 0.47$, $P < 0.0001$). Stability of visual acuity was observed with an average change of less than one letter ($n = 74$; OD −0.66 and OS −0.70 letters) in a mean follow-up time of 6.8 years. There was no statistically significant change in the ERG b/a ratio within eyes over time.

Conclusions. Although a broad spectrum of clinical phenotypes is observed across individuals with XLRS, our study demonstrates a significant correlation of structural and functional findings between the two eyes and stability of measures of acuity and ERG parameters over time. These results highlight the utility of the fellow eye as a useful reference for monocular interventional trials.

Keywords: X-linked retinoschisis, natural history, longitudinal

X-linked retinoschisis (XLRS) typically presents in boys with reduced visual acuity and findings of spoke-like configuration of intraretinal cysts at the fovea, sometimes accompanied by peripheral bullous retinal schisis changes.[1,2] Electrophysiologic testing demonstrates a characteristic reduction in b-wave amplitude relative to a-wave amplitude,[3] although exceptions occur.[4] The advent of optical coherence tomography (OCT) has advanced the visualization of the anatomic structural changes of the macula that characterize this disease and has aided in its diagnosis.[5–10] With identification of the *RS1* gene,[11,12] the retinoschisin protein was identified and found to have an evolutionarily conserved discoidin domain that provided insights into the function of this gene product in the retina.[3,13,14] Ongoing studies strive to elucidate the effects of protein mutations on retina structure and function.[15–17] Adding to the complexity is the considerable range of severity observed within a single family.[18] An effect of age also has been observed on central macular changes and clearly contributes to the slowly progressive phenotype.[17,19,20]

Herein, we examined the outcomes of structural and functional evaluation of 120 boys and men with XLRS who carry confirmed *RS1* mutations. We explored the correlation between the two eyes of a given participant as well as changes in vision and ERG parameters over time. Understanding the correlation of structural and functional parameters of the two eyes of a given patient will provide important information, critical to the design and outcome measures of future interventional studies.

Materials and Methods

Subjects

Examinations of 120 men and boys with bilateral clinical findings of XLRS and an identified *RS1* mutation were included. Of the 120 participants evaluated in the Ophthalmic Genetics Clinic of the National Eye Institute, 80 had additional follow-up visits in the range of 3 months to 47 years (mean = 6.67 ± 8.46 years). Fifty-five of the 80 participants underwent electrophysiological testing and 29 of those had at least 3 years of follow-up with ERG recordings.

This study adhered to the tenets of the Declaration of Helsinki for research involving human subjects and was approved by National Institutes of Health Neuroscience Institutional Review Board. Each subject gave written informed

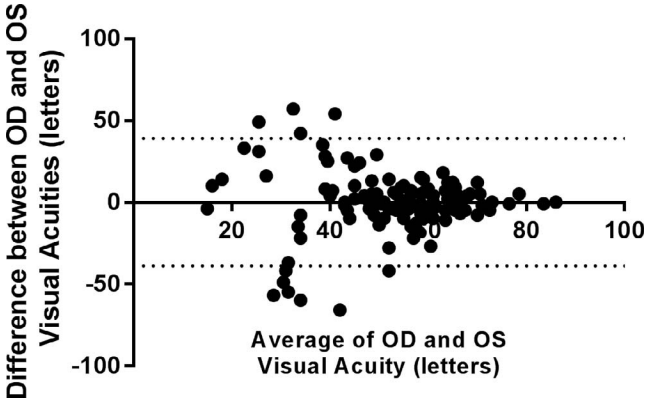

Figure 1. Representative Bland-Altman plot of visual acuity measurements of left and right eyes of patients with XLRS. *Solid line*: the bias (average mean difference) is 0.1; *dotted lines*: 95% confidence limits of agreement (–38.92 to 39.12).

consent after an explanation of the nature and possible consequences of the study.

Ocular Examinations

Study participants were assessed with a review of examination records, medical and ocular histories, slit-lamp biomicroscopy, and a dilated funduscopic examination. Best-corrected visual acuity was measured using the Early Treatment of Diabetic Retinopathy Study (ETDRS) chart recorded as the number of letters read or appropriate pediatric vision testing including Teller Acuity Cards, Allen figures, and/or HOTV charts.

Optical Coherence Tomography

Spectral-domain OCT (SD-OCT; Cirrus HD-OCT software version 9.5.0.8712, 2016; Carl Zeiss Meditec, Dublin, CA, USA) imaging was obtained in both eyes of 80 participants to capture a 512 × 128 scan pattern with the center of the nominal 6 × 6-mm scanning area positioned at the center of the macula. Quantitative longitudinal analysis of OCT scans was performed by first aligning the scans spatially using functions provided within the OCT instrument software (Carl Zeiss) and then checking for accuracy. The accuracy of automated delineations of the inner and outer retinal boundaries was also manually reviewed and verified for acceptability. OCT retinal thickness measurements in the macula were analyzed using a circular ETDRS-type grid positioned on the center of the fovea. Mean central macular thickness (CMT) measurements were calculated for the central subfield (central circle of approximately 1-mm diameter).

Electroretinography

Following pupil dilation, and 30 minutes of dark adaptation, International Society for Clinical Electrophysiology of Vision (ISCEV) standard full-field flash ERGs were recorded from corneal bipolar Burian-Allen electrodes (Hansen Ophthalmic Laboratories, Iowa City, IA, USA) using a commercial electrophysiology system (LKC, Gaithersburg, MD, USA). An Ag/AgCl electrode placed on the forehead served as ground.[21,22] Because the ERG b-wave is broad and the peak poorly defined in many XLRS subjects, we measured the amplitude of the ERG b-wave at a set implicit time of 47 ms that corresponds to the mean b-wave implicit time for healthy subjects with our ERG system (47 ms post flash; vertical dotted lines).[23]

Table 1. Characteristics of Patients With More Than 15 Letters Difference in Visual Acuity Between the Two Eyes

Characteristic	*n*	%
Strabismus	12	42.9
Laser/scarring/demarcation line in macula	5	17.9
History of vitreous hemorrhage	5	17.9
History of retinal detachment	3	10.7
Corneal opacification	1	3.6
Bullous schisis involving macula	1	3.6
Colobomatous macular lesion	1	3.6

RS1 Mutation Analysis

Genomic DNA was extracted from peripheral blood leukocytes and all six *RS1* exons and flanking intronic sequences were amplified by PCR using primers previously described.[11] Bidirectional sequence was analyzed for disease-causing mutations.

Analyses

We investigated the correlation between the two eyes both in structure with OCT, and function using both central visual acuity and ERG measurements. Participant age at the visit date was used in all analyses. In patients for whom longitudinal data were available, visual acuity and electroretinographic parameters were compared as a function of time. Statistical analyses and correlations between two variables were performed by using nonparametric correlations, paired *t*-test analysis, and linear regression implemented by GraphPad Prism (GraphPad Software, La Jolla, CA, USA).

Results

Subjects

The average age at initial examination was 22.4 years and ranged from 2.8 to 66.7 years. All 120 participants (92 families) underwent genetic testing and were found to have mutations in *RS1* (Supplementary Table S1). Of the 54 different mutations identified, 33 (61.1%) were missense mutations, 3 (5.6%) nonsense, 7 (13.0%) small deletions, 1 (1.9%) duplication, 2 (3.7%) indels, 3 (5.6%) gross deletions, and 5 (9.3%) splicing mutations. Three novel mutations were identified and are highlighted in bold in the Supplementary Table S1. Three patients

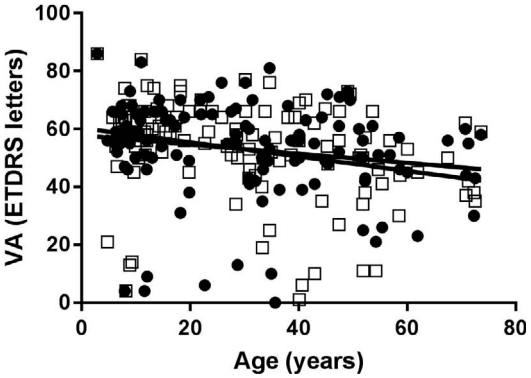

Figure 2. Scatter plot of visual acuity and age. Each data point represents the visual acuity as measured in number of letters read on the ETDRS chart for the right (*black dot*) ($P = 0.047$) and left (*open square*) ($P = 0.002$) eyes. *Solid lines* represent the linear regression fits for each eye.

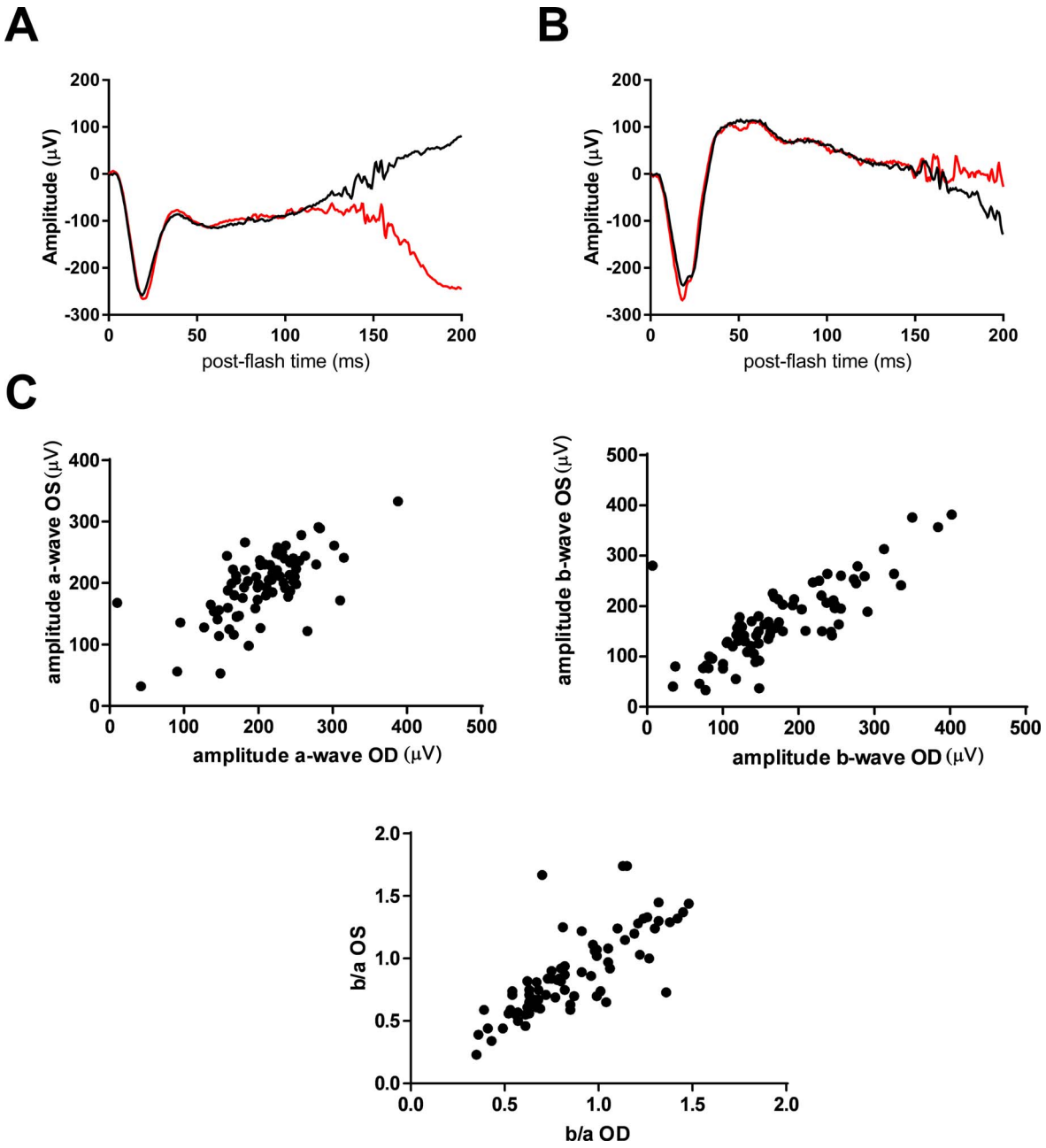

Figure 3. Correlation of electrophysiologic data between eyes. (**A**, **B**) Scotopic responses to a 2.4 cd-s/m^2 flash stimulus from two different participants; *black tracing* (right eye), *red tracing* (left eye). (**A**) Classically electronegative waveform with b-wave smaller than the a-wave. (**B**) Reduced b-wave that is not technically electronegative. The waveforms of each individual are qualitatively and quantitatively similar between eyes, but are different among participants. (**C**) Scatter plots of a-wave amplitude, b-wave amplitude, and b-/a-wave ratios measured in each eye of each of the 78 participants with ERG data.

were using topical dorzolamide 2% three times per day in both eyes at the time of their visit. Thirteen patients had retinal detachments (10.8%) and 14 vitreous hemorrhage (11.7%).

Correlation of Functional Measures Between Eyes

Visual Acuity. Visual acuities of right and left eyes of all 120 participants were compared using a nonparametric Spearman analysis and found to be correlated (Spearman $r = 0.47$, $P < 0.0001$). A Bland-Altman plot in Figure 1 illustrates the degree of agreement between eyes with a systematic bias of 0.1. Participants with average right and left eye acuities of fewer than 40 letters (20/160) demonstrated greater acuity differences between eyes. Visual acuities between the two eyes differed by fewer than 15 letters in 92 of the 120 participants (76.7%). In 28 patients (23.3%), there was more than a 15-letter difference between eyes, and their characteristics suggest a range of underlying etiologies (Table 1). When evaluating the entire cohort, there was no correlation between age at visit and difference in acuity between eyes (Spearman $r = 0.08$, $P = 0.37$). We do note a trend of worse visual acuity in both right and left eyes with increased age (slope –0.16 ± 0.08 and –0.25 ± 0.08 letters per year of age respectively) (Fig. 2).

Electrophysiology. Functional analysis of the ERG focused on the ISCEV dark-adapted response to a 2.4 cd-s/m^2 stimulus flash that elicits a-wave activity from rod photorecep-

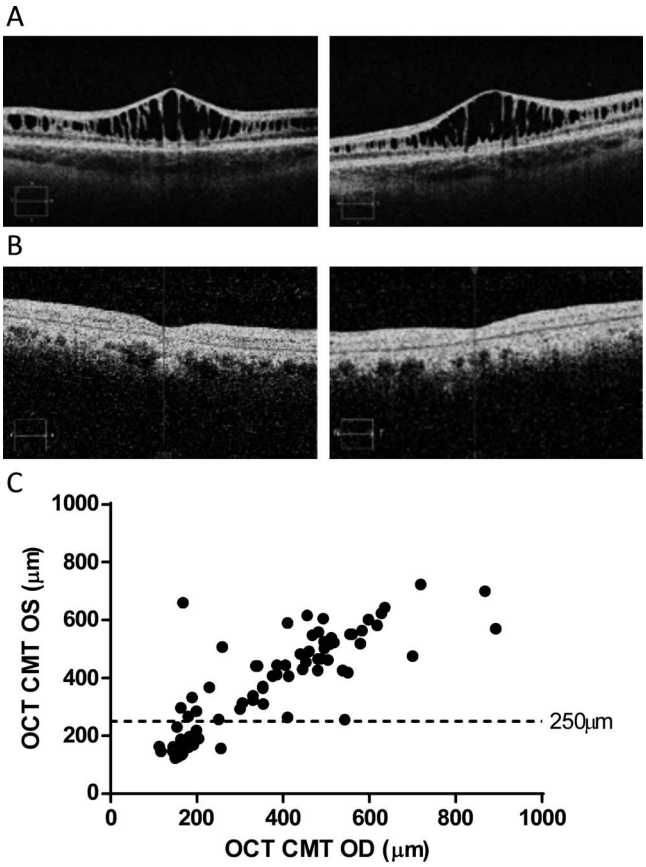

FIGURE 4. SD-OCT scans through the fovea of two different XLRS participants. (**A**) Participant 1: demonstrating classic schisis cavities in macula OU. (**B**) Participant 2: showing atrophy and no schisis cavities. Right and left eyes demonstrate similar characteristics within the same patient, however the OCT findings of participant 1 differ significantly from participant 2. (**C**) Scatter plot of the right and left eye central OCT measurements with a "normal" OCT CMT[35,36] (250 μm) indicated with a *dashed line*.

tors and typically reveals characteristic "electronegative waveform" (Fig. 3A) frequently associated with XLRS, although exceptions occur (Fig. 3B). Seventy-eight participants had ERG recording performed on both eyes. Amplitudes of the a- and b-waves, and also the b-/a-wave amplitude ratio, demonstrated significant correlation between the two eyes (Fig. 3C; a-wave: Spearman $r = 0.63$; b-wave: $r = 0.78$; b/a-wave: $r = 0.82$; $P < 0.0001$ for all three parameters). We also observed a weak correlation between visual acuity and b/a-wave ratio (OD Spearman $r = 0.42$, $P = 0.0001$; OS Spearman $r = 0.37$, $P = 0.0007$).

Correlation of Structural Measures Between Eyes

Central Structure as Measured Using CMT on Spectral-Domain OCT. CMTs of the right and left eyes were obtained for 80 participants and were found to be qualitatively similar between eyes. Although substantial structural differences are found between XLRS individuals (Fig. 4A versus 4B), the qualitative differences between the two eyes of any individual were usually relatively small. Central thickness of the two eyes of a given participant was highly correlated on OCT measurement (Spearman $r = 0.83$, 95% confidence interval 0.75–0.89, $P < 0.0001$; Fig. 4C). And, as can be seen in Figure 4C, most (69%) eyes have a CMT greater than the 250 μm in at least one eye.

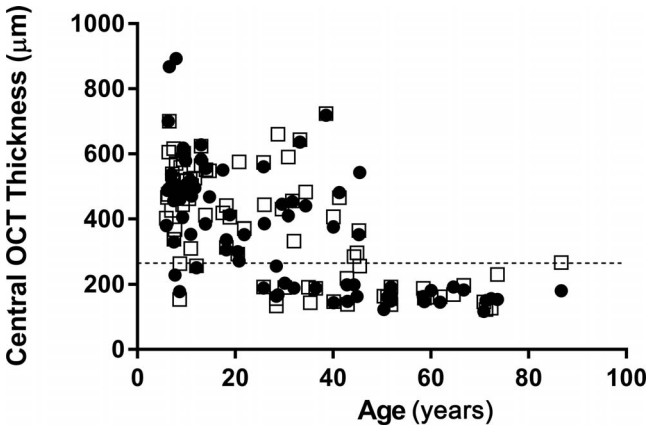

FIGURE 5. Scatter plot of the central OCT thickness and age. Each data point represents the central OCT thickness for the right (*black dot*) and left (*open square*) eyes. Of the 15 individuals older than 45 years, 93% showed pathologic thinning of macular neural tissue.

CMT Versus Age. Although cystic changes seem almost pathognomonic for diagnosing XLRS disease, these are not always seen in the older affected population. Menke et al. noted that individuals with XLRS older than 45 showed macular atrophy on OCT.[19] Others have now confirmed this age-related finding of foveal thinning that occurs with increasing age.[20] In our cohort, 93% (28 of 30 eyes) of the 15 individuals older than 45 years showed pathologic thinning of macular neural tissue defined as central OCT thickness less than 250 μm (Fig. 5). There was no statistically significant correlation between OCT CMT and visual acuity in this subgroup of patients.

Longitudinal Changes

Visual Acuity. Seventy-three patients in this cohort had visual acuity data for two or more time points (Table 2). The mean change in visual acuity was –0.66 and –0.70 letters in the right and left eye, respectively (average rate of change of –0.22 letters across both eyes per year), over a mean follow-up of 6.8 years (range, 2 months to 47 years). Most eyes had a change in visual acuity of 5 or fewer letters, and only three eyes (2.1%) worsened by 15 letters or more (Fig. 6). Our analysis of visual acuity at first visit and final follow-up visit did not reveal a statistically significant change in acuity in either eye, demonstrated by a lack of significant difference on paired *t*-test analysis (OD $P = 0.65$, OS $P = 0.22$) and strong correlation between measurements with Spearman *r* of 0.86 OD and 0.79 OS, $P < 0.0001$. Three participants had a documented decrease in visual acuity of 15 letters or more in one eye with a mean

TABLE 2. Change in Visual Acuity (VA) Since Initial Visit, by Age

Age at Initial Visit, y	No. of Patients	VA at Initial Visit, Mean, Letters		Average Follow-up, y	ΔVA From Initial Visit, Mean, Letters	
		OD	OS		OD	OS
<10	28	56.6	53.1	7.9	0.6	1.3
10–19	9	57.6	55.6	8.0	−1.8	−0.7
20–29	13	54.3	53.5	5.8	−2.6	−2.6
30–39	6	43.3	54.5	6.8	0.2	−2.5
40–49	13	58.2	52.8	5.3	−0.1	−1.3
50–59	1	55.0	59.0	4.6	6.0	7.0
60–69	3	57.0	53.7	5.8	−4.0	−4.7

Table 3. Change in Visual Acuity (VA) Since Initial Visit by Length of Follow-up

Length of Follow-up, y	No. of Patients	ΔVA From Initial Visit, Mean, Letters		Average Age at Final Visit, y
		OD	OS	
<1	7	0.0	−0.4	19.8
1–3	20	−0.3	2.6	22.6
3–5	16	0.5	−0.4	28.8
5–10	19	−0.7	−1.4	35.0
10–30	7	−3.4	−8.6	37.7
>30	4	−3.0	−1.8	47.2

age of 11.2 years at initial visit (range, 5.4 to 20.1 years) and an average of 18.7 years of follow-up (Supplementary Table S2). Two of these patients were 8 years or younger at the first visit and could not participate in ETDRS testing; their visual acuity was measured with Allen figures and HOTV charts, which may lead to an overestimation of acuity loss when compared with the more accurate ETDRS measurement taken at the follow-up visit. When the data are grouped by time of follow-up (Table 3), we can see a trend for long times (more than 10 years) of follow-up visual acuity on average drifting downward to an average worsening of 3 to 8 letters.

Electrophysiology. The rate of change in ERG parameters was calculated in participants with ERGs recorded at three or more visits from the linear fit of the data plotted at a function of the duration of follow-up. Participants with at least 3 years of follow-up ($n = 20$) and at least 5 years of follow-up ($n = 17$) were analyzed. As demonstrated in Table 4, 30-Hz latency slowed with time ($P = 0.02$) over 3 years. However, when calculating rate of change in patients with 5 years of follow-up, there was no statistically significant difference in the rate of change in any ERG parameter (Table 3). When comparing only the first and most recent visit, the results were largely the same, with no statistically significant change in the ERG parameters for those with at least 5 years of follow-up (Supplementary Table S3).

Discussion

Here we report on a large cohort of participants with confirmed *RS1* mutations and examine the symmetry between eyes in the outcome measures of acuity, OCT, and ERG.

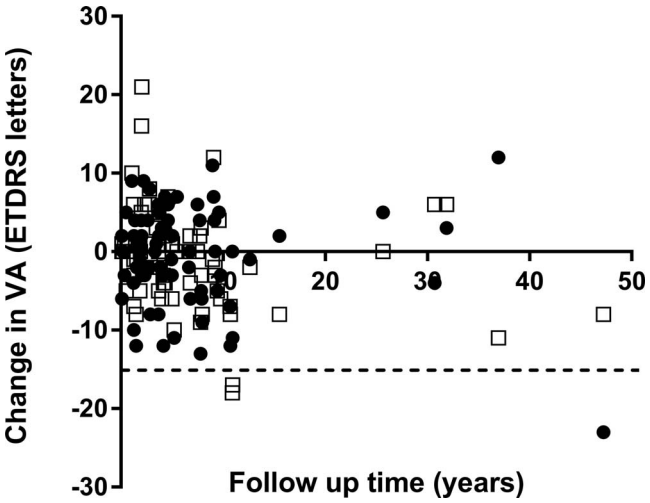

Figure 6. Scatter plot of the change in measured visual acuity and follow-up time in years. Each data point represents the visual acuity as measured in number of letters read on the ETDRS chart for the right (*black dot*) and left (*open square*) eyes.

Previous publications have pointed to the spectrum of disease phenotype observed across individuals with XLRS. In those studies, a variety of factors were thought to contribute to the spectrum of clinical manifestations observed, including underlying genetic mutation[17] and age, among others.[17–19,24,25] By limiting our analysis to the comparison of the two eyes of a given participant, we inherently keep these known and unknown variables constant and find that the characteristics of one eye mirror the structural and functional findings in the fellow eye in highly predictable fashion.

Some have noted that the classic clinical finding of central cystic changes that seem almost pathognomonic for diagnosing the disease are not necessarily seen in the older population.[19] CMT ranged from 117 to 868 μm in this study, and the knowledge of the thickness in one eye highly predicted the CMT findings in the fellow eye, with a value of $r = 0.83$. In a similar manner, the electronegative b-wave that is often discussed as the electrophysiologic signature of this disease is quantitatively variable, with all patients demonstrating a reduced b/a ratio, but not all reaching the definition of electronegative. Although there is a large spectrum of the degree to which the b-wave is reduced relative to the a-wave

Table 4. The Rate of Change in ERG Parameters in Patients With Three or More Follow-up Visits Showed No Statistically Significant Correlations Except for 30-Hz Latency ($P = 0.02$) Over 3 Years; However, This Was Not Consistent With Analysis of 5-Year Follow-up Data

ERG Parameter	>3-y Follow-up and 3 or More Visits, $n = 20$		>5-y Follow-up and 3 or More Visits, $n = 17$	
	Mean ± SD	*P*	Mean ± SD	*P*
a-wave amplitude, log μV/y	−0.005 ± 0.020	0.31	0.002 ± 0.012	0.49
b-wave amplitude, log μV/y	−0.001 ± 0.026	0.92	0.008 ± 0.017	0.08
Photopic amplitude, log μV/y	0.006 ± 0.018	0.14	−0.003 ± 0.017	0.42
30-Hz amplitude, log μV/y	−0.009 ± 0.024	0.13	−0.003 ± 0.017	0.50
b/a ratio, per year	0.007 ± 0.024	0.24	0.009 ± 0.025	0.16
Photopic latency, ms/y	−0.020 ± 0.156	0.57	0.021 ± 0.154	0.59
30-Hz latency, ms/y	0.123 ± 0.222	0.02*	0.081 ± 0.161	0.055
Statistics of visits	• Median follow-up = 7.8 y; range = 3.0 to 12.3 y • Median number of visits = 3.5; range = 3 to 7 visits • Mean age at baseline visit = 35.0 y; range = 7.5 to 62.0 y		• Median follow-up = 9.3 y; range = 5.7 to 12. 3 y • Median number of visits = 4; range = 3 to 7 visits • Mean age at baseline visit = 32.0 y; range = 7.5 to 62.0 y	

* $P < 0.05$.

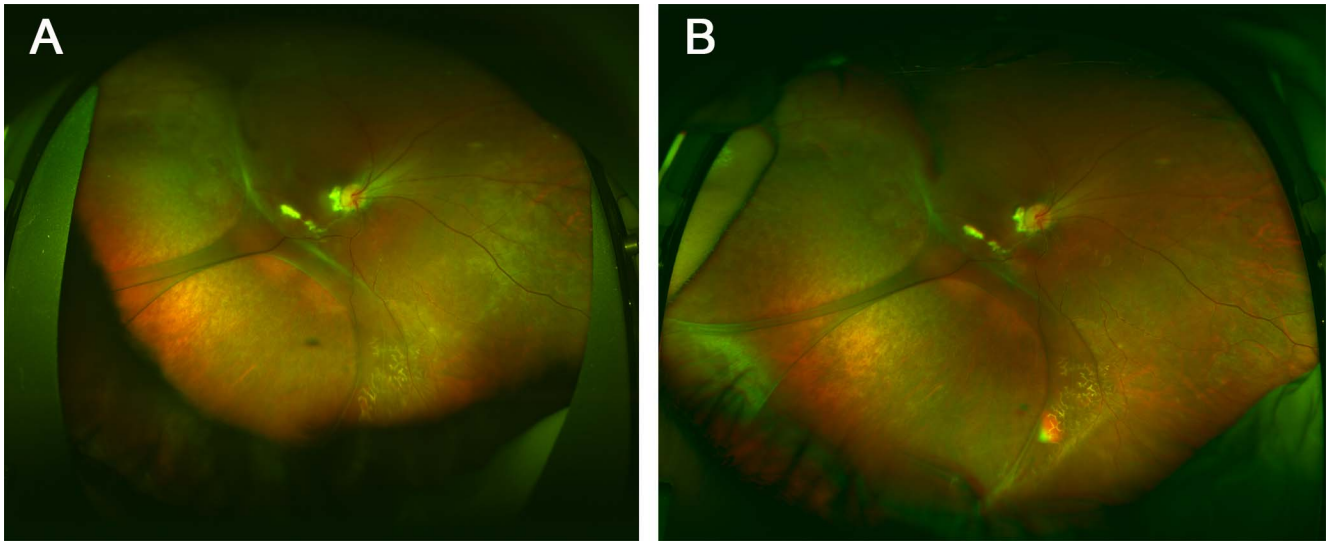

FIGURE 7. Optos imaging of the right eye of a patient at age 19 years with visual acuity (VA) 20/40 (*left*), and 24 years, VA 20/40 (*right*), demonstrating stability of large bullous schisis anatomic features.

across patients (b/a ratio range, 0.23–1.7), we demonstrate here that the two eyes of a patient with XLRS are highly correlated (r value = 0.80) with highly similar reductions in their b-wave relative to a-waves.

The clinical phenotype of XLRS patients has been described since 1898[26] and yet few have reported on the long-term follow-up of this cohort. To our knowledge, this is the largest published cohort of patients with molecularly proven XLRS with long-term follow-up. Consistent with other investigators who have evaluated visual acuity longitudinally in patients with XLRS, we find relatively stable measures at different time points (Fig. 7) unless severe complications occurred.[27] Frequency of complications, such as vitreous hemorrhage and retinal detachment have been reported by George et al.,[28] Kellner et al.,[29] Roesch et al.,[30] and most recently Fahim et al.[31] In our cohort, we identified retinal detachment in 10.8% of patients and vitreous hemorrhage in 11.7%; only three patients had a history of both retinal detachment and vitreous hemorrhage. This is comparable, although on the lower end of the range of 3% to 21% vitreous hemorrhage and 5% to 40% retinal detachment reported in the literature.[28–32] Of the participants who had a more than 15-letter difference between eyes, several had strabismus or structural macular changes that could contribute to this decreased visual acuity. Any structural or functional disparity between eyes has the potential to lead to amblyopia, and the contribution of developmental visual loss is impossible to separate completely from any biologic disparity. The presence of strabismus suggests a component of amblyopia that could be contributing to the asymmetry in visual acuity between eyes. The impact of age and accuracy of initial visual acuity also must be considered in the group of patients who demonstrated a loss of 15 letters or more over time. We also find stable ERG parameters when patients are followed longitudinally. Although there was an increase in 30-Hz latency in patients with three visits and at least 3 years of follow-up, this statistical change was not maintained when analyzed in patients with at least 5 years of follow-up (Table 4).

Currently there are no treatments approved by the Food and Drug Administration for patients with XLRS, but with successful preclinical studies in mouse models[33,34] and multiple Phase I/II clinical trials involving AAV-mediated gene therapy under way, it is imperative to understand the natural progression of disease when choosing outcome measures for an interventional study. Our findings indicate that, given the same mutation in the same biologic milieu of an individual, the structure and function of the retina in the two eyes is similar. That is, barring accidental injury to one eye, including the infrequent occurrence of a retinal detachment, or the presence of strabismus, one can conclude visual acuity, CMT on OCT, and electrophysiologic measures are quite comparable between eyes and will likely remain that way over time. These results highlight the potential for monocular treatments to use the fellow eye as an appropriate comparison reference. The finding of a strong correlation of structural and functional measures between the two eyes of a given participant as well as the stability of these measures over time will undoubtedly prove useful for analyses involving a uniocular intervention.

Acknowledgments

Supported by funds from the National Eye Institute Intramural Research Program.

Disclosure: **C.A. Cukras**, None; **L.A. Huryn**, None; **B.G. Jeffrey**, None; **A. Turriff**, None; **P.A. Sieving**, None

References

1. Sieving PA, MacDonald IM, Chan S. X-linked juvenile retinoschisis. In: Adam MP, Ardinger HH, Pagon RA, et al., eds. *GeneReviews®*. Seattle: University of Washington, Seattle; 1993–2018. Available at: https://www.ncbi.nlm.nih.gov/books/NBK1222/.
2. Molday RS, Kellner U, Weber BHF. X-linked juvenile retinoschisis: clinical diagnosis, genetic analysis, and molecular mechanisms. *Prog Retin Eye Res*. 2012;31:195–212.
3. Khan NW, Jamison JA, Kemp JA, Sieving PA. Analysis of photoreceptor function and inner retinal activity in juvenile X-linked retinoschisis. *Vision Research* 2001;41:3931–3942.
4. Sieving PA, Bingham EL, Kemp J, Richards J, Hiriyanna K. Juvenile X-linked retinoschisis from XLRS1 Arg213Trp mutation with preservation of the electroretinogram scotopic b-wave. *Am J Ophthalmol*. 1999;128:179–184.
5. Prenner JLM, Capone AJM, Ciaccia SM, Takada YM, Sieving PAM, Trese MTM. Congenital X-linked retinoschisis classification system. *Retina*. 2006;26:S61–S64.

6. Eriksson U, Larsson E, Holmström G. Optical coherence tomography in the diagnosis of juvenile X-linked retinoschisis. *Acta Ophthalmol Scand*. 2004;82:218–223.
7. Chan WM, Choy KW, Wang J, et al. Two cases of X-linked juvenile retinoschisis with different optical coherence tomography findings and RS1 gene mutations. *Clin Exp Ophthalmol*. 2004;32:429–432.
8. Stanga PE, Chong NHV, Reck AC, Hardcastle AJ, Holder GE. Optical coherence tomography and electrophysiology in X-linked juvenile retinoschisis associated with a novel mutation in the XLRS1 gene. *Retina*. 2001;21:78–80.
9. Gregori NZ, Berrocal AM, Gregori G, et al. Macular spectral-domain optical coherence tomography in patients with X linked retinoschisis. *Br J Ophthalmol*. 2009;93:373–378.
10. Gregori NZ, Lam BL, Gregori G, et al. Wide-field spectral-domain optical coherence tomography in patients and carriers of X-linked retinoschisis. *Ophthalmology*. 2013;120: 169–174.
11. Sauer CG, Gehrig A, Warneke-Wittstock R, et al. Positional cloning of the gene associated with X-linked juvenile retinoschisis. *Nat Genet*. 1997;17:164–170.
12. Sieving PA, Yashar BM, Ayyagari R, et al. Juvenile retinoschisis: a model for molecular diagnostic testing of X-linked ophthalmic disease. *Trans Am Ophthalmol Soc*. 1999;97:451–469.
13. Takada Y, Fariss RN, Müller M, Bush RA, Rushing EJ, Sieving PA. Retinoschisin expression and localization in rodent and human pineal and consequences of mouse RS1 gene knockout. *Mol Vis*. 2006;12:1108–1116.
14. Johnson BA, Ikeda S, Pinto LH, Ikeda A. Reduced synaptic vesicle density and aberrant synaptic localization caused by a splice site mutation in the Rs1h gene. *Vis Neurosci*. 2006;23: 887–898.
15. Sergeev YV, Caruso RC, Meltzer MR, Smaoui N, MacDonald IM, Sieving PA. Molecular modeling of retinoschisin with functional analysis of pathogenic mutations from human X-linked retinoschisis. *Hum Mol Genet*. 2010;19:1302–1313.
16. Sergeev YV, Vitale S, Sieving PA, et al. Molecular modeling indicates distinct classes of missense variants with mild and severe XLRS phenotypes. *Hum Mol Genet*. 2013;22:4756–4767.
17. Bowles K, Cukras C, Turriff A, et al. X-linked retinoschisis: RS1 mutation severity and age affect the ERG phenotype in a cohort of 68 affected male subjects. *Invest Ophthalmol Vis Sci* 2011;52:9250–9256.
18. Eksandh LC, Ponjavic V, Ayyagari R, et al. Phenotypic expression of juvenile x-linked retinoschisis in Swedish families with different mutations in the xlrs1 gene. *Arch Ophthalmol*. 2000;118:1098–1104.
19. Menke MN, Feke GT, Hirose T. Effect of aging on macular features of X-linked retinoschisis assessed with optical coherence tomography. *Retina*. 2011;31:1186–1192.
20. Andreoli MT, Lim JI. Optical coherence tomography retinal thickness and volume measurements in X-linked retinoschisis. *Am J Ophthalmol*. 2014;158:567–573.e2.
21. Marmor MF, Fulton AB, Holder GE, Miyake Y, Brigell M, Bach M. ISCEV Standard for full-field clinical electroretinography (2008 update). *Doc Ophthalmol*. 2009;118:69–77.
22. McCulloch DL, Marmor MF, Brigell MG, et al. ISCEV Standard for full-field clinical electroretinography (2015 update). *Doc Ophthalmol*. 2015;130:1–12.
23. Jeffrey BG, Cukras CA, Vitale S, Turriff A, Bowles K, Sieving PA. Test–retest intervisit variability of functional and structural parameters in X-linked retinoschisis. *Trans Vis Sci Tech*. 2014;3(5):5.
24. Lesch B, Szabó V, Kánya M, et al. Clinical and genetic findings in Hungarian patients with X-linked juvenile retinoschisis. *Mol Vis*. 2008;14:2321–2332.
25. Apushkin MA, Fishman GA, Rajagopalan AS. Fundus findings and longitudinal study of visual acuity loss in patients with X-linked retinoschisis. *Retina*. 2005;25:612–618.
26. Haas J. Über das Zusammen Vorkommen von Veränderungen der Retina und Choroidea. *Arch Augenheilkd*. 1898;37:343–348.
27. Kjellström S, Vijayasarathy C, Ponjavic V, Sieving PA, Andréasson S. Long-term 12 year follow-up of X-linked congenital retinoschisis. *Ophthalmic Genet*. 2010;31:114–125.
28. George ND, Yates JR, Moore AT. Clinical features in affected males with X-linked retinoschisis. *Arch Ophthalmol*. 1996; 114:274–280.
29. Kellner U, Brümmer S, Foerster MH, Wessing A. X-linked congenital retinoschisis. *Graefes Arch Clin Exp Ophthalmol*. 1990;228:432–437.
30. Roesch MT, Ewing CC, Gibson AE, Weber BH. The natural history of X-linked retinoschisis. *Can J Ophthalmol*. 1998;33: 149–158.
31. Fahim AT, Ali N, Blachley T, Michaelides M. Peripheral fundus findings in X-linked retinoschisis. *Br J Ophthalmol*. 2017;101: 1555–1559.
32. Peachey NS, Fishman GA, Derlacki DJ, Brigell MG. Psychophysical and electroretinographic findings in X-linked juvenile retinoschisis. *Arch Ophthalmol*. 1987;105:513–516.
33. Bush RA, Zeng Y, Colosi P, et al. Preclinical dose-escalation study of intravitreal AAV-RS1 gene therapy in a mouse model of X-linked retinoschisis: dose-dependent expression and improved retinal structure and function. *Hum Gene Ther*. 2016;27:376–389.
34. Kjellstrom S, Bush RA, Zeng Y, Takada Y, Sieving PA. Retinoschisin gene therapy and natural history in the Rs1h-KO mouse: long-term rescue from retinal degeneration. *Invest Ophthalmol Vis Sci*. 2007;48:3837–3845.
35. Hagen S, Krebs I, Haas P, et al. Reproducibility and comparison of retinal thickness and volume measurements in normal eyes determined with two different Cirrus OCT scanning protocols. *Retina*. 2011;31:41–47.
36. Liu T, Hu AY, Kaines A, Yu F, Schwartz SD, Hubschman JP. A pilot study of normative data for macular thickness and volume measurements using Cirrus high-definition optical coherence tomography. *Retina*. 2011;31:1944–1950.

Investigative Ophthalmology & Visual Science